

Proceedings of the Fifth International Conference on
Railway Technology:
Research, Development and Maintenance
Edited by J. Pombo
Civil-Comp Conferences, Volume 1, Paper 20.9
Civil-Comp Press, Edinburgh, United Kingdom, 2022, doi: 10.4203/ccc.1.20.9
©Civil-Comp Ltd, Edinburgh, UK, 2022

On the influence of ballast fouling materials and compaction states on the dynamic cone resistance

Sébastien Barbier¹, Jorge Rojas Vivanco¹, Miguel Angel Benz Navarrete¹, Younes Haddani¹

¹Sol Solution, France

Abstract

This work presents the results of tests carried out as part of the study of the influence of ballast fouling materials and compaction states on the dynamic cone resistance. It is a complement for a previous study on the statistical analysis of the influence of ballast fouling on penetrometer and geoendoscope data [1].

As a result of this previous work, a particular behaviour of the average cone resistance was highlighted. The cone resistance (q_d) initially increases with Fouling Index, highlighting the mechanical resistance to penetration improvement of the ballasted layer. Then, when the ballast is fouled, this mechanical resistance decreases. However, the tests cases This behaviour was highlighted for specimens without compaction differences.

The present study exposes results obtained from similar test specimens compacted in two new distinct sates. For the same range of Fouling Index (FI), this study confirms the previously highlighted behavior for more compacted test cases with only sandy fouling material.

Keywords: Fouling index, Compaction, Dynamic cone resistance, Ballasted layer.

1 Introduction

This work is a complement for a previous study on the statistical analysis of the influence of ballast fouling on penetrometer and geoscope data [1]. Most of rail networks around the world are often composed of ballasted tracks, where the main component is the “ballast”. Over time and as a result of repeated and increasing heavy loads the railway track ages, and the ballast deteriorates deviating from its original standard specifications. As a result, the ballast layer is progressively fouled with materials finer than aggregate particles, filling the void spaces. Fouled ballast impacts the track performance by changing the mechanical properties of sub-structure layers. Field characterization of ballast fouling degree as well as its mechanical behavior is an important task to optimize decision making in railways tracks maintenance programs.

The French lightweight dynamic penetrometer, known as P.A.N.D.A test [2], coupled with geoscope [3-4] offers the opportunity to reach this purpose by measuring the dynamic cone resistance (q_d) and image features continuously in depth (Fig. 1). This method has been widely studied to evaluate the bearing capacity as well as to assess mechanical properties of the soil layers. A previous study focused on establishing a relationship between (q_d), images parameters and ballast fouling index (FI). Previously analysed data were obtained from specimens with the same compaction state. This study presents complementary results obtained from specimens in distinct compaction states.

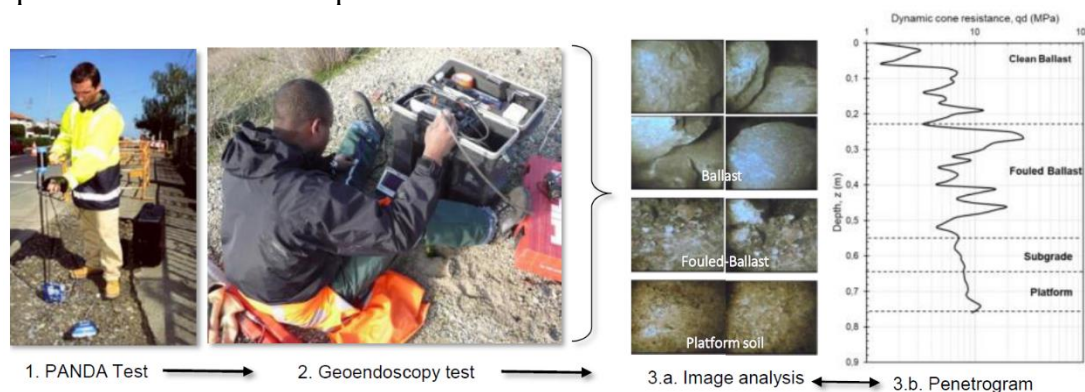


Figure 1: Principle of lightweight dynamic penetrometer P.A.N.D.A and Geoscope tests

This article presents parts of the results obtained from a laboratory study aimed at establishing a database to correlate dynamic penetrometer values, images features as well as GPR data in order to improve railroad surveys by means of data fusion. This study is particularly interested in the effects of compaction on the measured cone resistance.

2 Methods

The same type of parallelepipedal specimens of soil (800x600x1000mm) as in the previous study [1] were prepared (Figure 2). The main purpose is to reproduce a multi-layer structure representative of a railway track, where the lower part is the subgrade, and the upper part simulates the ballasted layer. Subgrade were designed by two different layers (silty-sand and clay) that remain unchanged in terms of

nature as well as compaction degree. In this study and for each sample, ballasted upper layer changes in content of fouling material and in compaction degree. Fouled ballast was created by mixing different quantities of clean ballast, and sand (only sand for this compaction effect study).

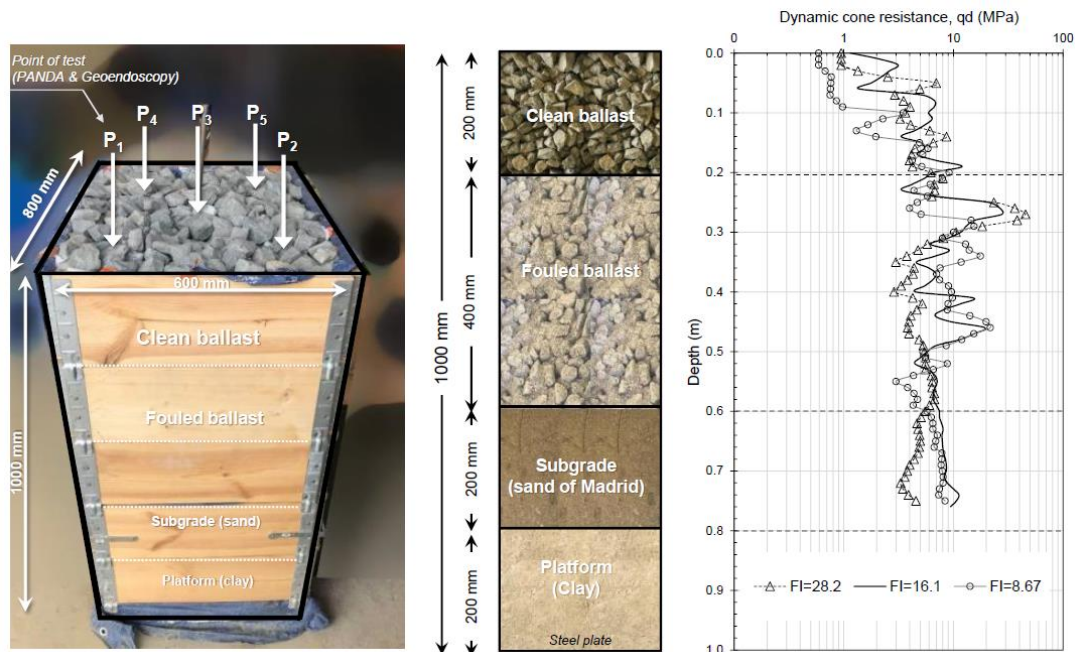


Figure 2: Laboratory experiences: (left) dimensions of specimens and test position; (middle) vertical profile of specimens tested; (right) example of dynamic penetration test results.

A total of 18 specimens were tested: 3 distinct compaction states for 6 fouling index (FI) conditions. The first compaction state is a state without compaction, called C0. For the other states, compaction is carried out using a compaction mass. The specimen is divided into 6 zones and for each zone 2 strokes of mass are given. This operation is repeated 4 times for the second case of compaction (C4) and 8 times for the third (C8). 5 Dynamic penetration and 5 geoscope tests, as well as GPR measurements were conducted for each sample. The goal of this experiment was to qualify the effects of compaction on the values measured by P.A.N.D.A. in order to complement the previous study [1].

Sample construction begins with the manual compaction of a 100mm thick subgrade soil layer. Geotextile is placed between each layer and the construction proceeds with the placement of each layer until the top layer (clean ballast) is reached. Once the tests are carried out, the specimen is completely emptied, and another sample is later built. Fouled ballast was prepared thanks to a concrete mixer and the mixture was placed inside the specimen in compacted layers. It should be noted that, vertical stress resulting from the weight applied by the superstructure of the railway (rail, sleepers etc) is not simulated in these experiences and should change the range of the measured values.

3 Results

For each specimen, five penetration tests were carried out and only the part of the signal obtained in the ballasted layer is analysed. Average value of cone resistance q_d are calculated for clean ballast and fouled ballast layers. Table 1 below summarize the test cases and results.

Table 1: Summary of different cases: Compaction state, Fouling Index (FI) and qd average values

| Compaction state | FI (%) | FI Class | qd mean (MPa) | qd std (MPa) | W% | Total mass (kg) | Density (kN/m ³) |
|---------------------|--------|----------|---------------|--------------|------|-----------------|------------------------------|
| Compaction state C0 | 0,0 | C | 5,6 | 4,7 | 0 | 290 | 15,5 |
| | 8,7 | MC | 8,1 | 4,4 | 5,98 | 293 | 15,2 |
| | 16,1 | MF | 9,3 | 5,6 | 5,8 | 315 | 16,4 |
| | 28,2 | F | 8,8 | 6,8 | 6,12 | 360 | 18,8 |
| | 37,6 | F | 6,9 | 4,3 | 5,3 | 360 | 18,8 |
| | 51,2 | HF | 3,9 | 3,3 | 5,72 | 385 | 20,1 |
| Compaction state C4 | 0,0 | C | 6,8 | 5,6 | 0 | - | - |
| | 8,7 | MC | 12,3 | 4,4 | 5,98 | 309 | 15,7 |
| | 16,1 | MF | 13,5 | 5,6 | 5,8 | 333 | 16,9 |
| | 28,2 | F | 14,9 | 6,8 | 6,12 | 380 | 19,3 |
| | 37,6 | F | 15,0 | 4,3 | 5,3 | 382 | 19,4 |
| | 51,2 | HF | 11,8 | 3,3 | 5,72 | 410 | 20,8 |
| Compaction state C8 | 0,0 | C | 9,0 | 6,7 | 0 | - | - |
| | 8,7 | MC | 14,9 | 4,4 | 5,98 | 309 | 16,1 |
| | 16,1 | MF | 15,9 | 5,6 | 5,8 | 333 | 17,3 |
| | 28,2 | F | 16,1 | 6,8 | 6,12 | 380 | 19,8 |
| | 37,6 | F | 15,8 | 4,3 | 5,3 | 382 | 19,9 |
| | 51,2 | HF | 13,3 | 3,3 | 5,72 | 410 | 21,3 |

C: Clean; MC: Moderately Clean; MF: Moderately Fouled; F: Fouled; HF: Highly Fouled.

Regarding compaction states, an increase in density and average cone resistance can be denoted for each FI cases. Results are also plotted in Figure 3. Where we can see a similar behavior for the three compaction states. It should be noted that the cone resistance values presented are much lower than those measured in practice [3-7]. Indeed, as mentioned above, the effects of overburden pressure (due to the track load) as well as rod's skin friction has been neglected.

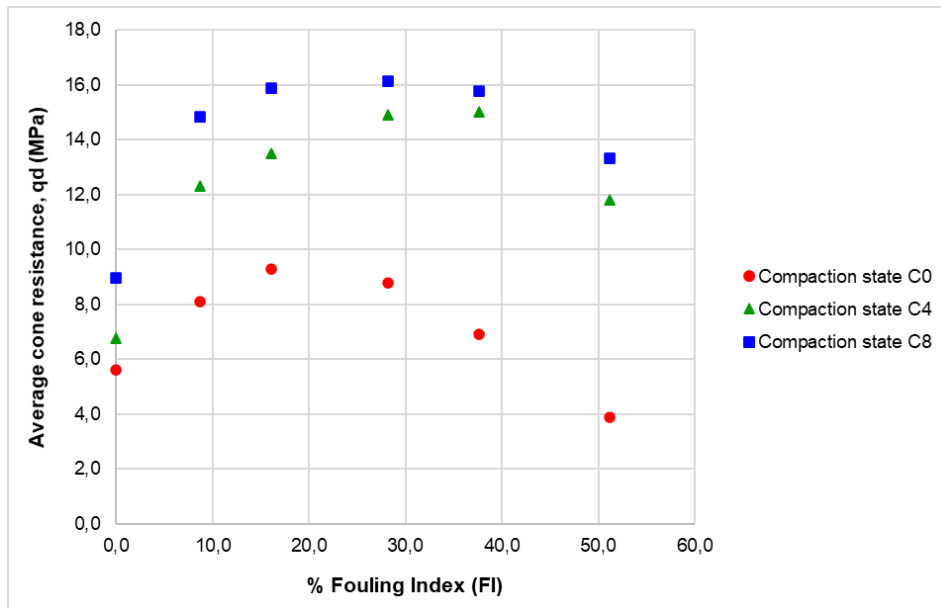


Figure 3: Evolution of dynamic cone resistance q_d according to fouling index for distinct compaction methods

The cone resistance initially increases with Fouling Index, highlighting the mechanical resistance to penetration improvement of the ballasted layer. Then, when the ballast is more fouled, this mechanical resistance decreases. This behaviour, highlighted in the previous study [1], is still present within C4 and C8. Regarding absolute values, the increase of resistance seems to be more important for greater compaction at low FI. The decrease at high FI seems to be less important at higher compaction degrees.

4 Conclusions and Contributions

Fouling in the ballast layers change the mechanical behavior of the railway tracks. In a previous study [1], the influence of ballast fouling quantity and material type on dynamic penetrometer and geodoscope tests results were analyzed. A particular behaviour of the average cone resistance was highlighted.

The cone resistance (q_d) initially increases with Fouling Index, highlighting the mechanical resistance to penetration improvement of the ballasted layer. Then, when the ballast is fouled, this mechanical resistance is smaller than that of the clean ballast. The nature of the fouling material changes the degree of the above effects: in the case of sandy soils the resistance is higher than that of clayey soils. This behaviour was highlighted for specimens without compaction differences. The present study exposes results obtained from similar test specimens compacted in two new distinct sates. For the same range of Fouling Index (FI), this study confirms the previously highlighted behavior for more compacted test cases with only sandy fouling material.

This study covers only one fouling material type and therefore cannot be generalized as it is. Moreover, the effects of overburden pressure due to the track load as well as

rod's friction has been neglected. Further experiments should be carried out to improve railway's tracks diagnostic through dynamic penetrometer data.

References

1. J. Rojas Vivanco, S. Barbier, M.A. Benz Navarrete, P. Breul (2022) Statistical Analysis of the Influence of Ballast Fouling on Penetrometer and Geoendoscope Data. In: Tutumluer E., Nazarian S., Al-Qadi I., Qamhia I.I. (eds) Advances in Transportation Geotechnics IV. Lecture Notes in Civil Engineering, vol 165. Springer, Cham.
2. R. Gourvès, “Pénétrömètre dynamique à energie variable,” Patent n° FR2817344, 2002.
3. Y. Haddani et al., “High yield geotechnical characterization of existing railway tracks,” Civil-Comp Proc., vol. 110, 2016.
4. Y. Haddani, P. Breul, G. Saussine, M. A. B. Navarrete, F. Ranvier, and R. Gourvès, “Trackbed Mechanical and Physical Characterization using PANDA®/Geoendoscopy Coupling,” Procedia Eng., vol. 143, no. Ictg, pp. 1201–1209, 2016.
5. G. Saussine, A. Dhemaied, Q. Delforge, and S. Benfeddoul, “Statistical analysis of cone penetration resistance of railway ballast,” EPJ Web Conf., vol. 140, pp. 2–5, 2017.
6. F. Lamas-Lopez, Y. J. Cui, S. Costa dAguiar, and N. Calon, “Geotechnical auscultation of a French conventional railway track-bed for maintenance purposes,” Soils Found., vol. 56, no. 2, pp. 240–250, 2016.
7. H. Kazmee, E. Tutumluer, Y. Haddani, M. A. Benz Navarrete, and R. Gourves, “Use of a Variable Energy Penetrometer and Geo-Endoscopic Imaging in the Performance Assessment of Working Platforms Constructed with Large Size Unconventional Aggregates,” in International Conference on Transportation and Development 2016: Projects and Practices for Prosperity - Proceedings of the 2016 International Conference on Transportation and Development, 2016, pp. 1227–1238.